J. Phys. Chem. A **2007,** *111,* 13193−13199 **13193**

Ab Initio Study of Low-Lying Electronic States of $SnCl_2^+$

Edmond P. F. Lee,[†,‡,§] John M. Dyke,[†] Wan-ki Chow,*[,‡] Daniel K. W. Mok,*[,§] and Foo-tim Chau*[,§]

Departments of Building Services Engineering and Applied Biology and Chemical Technology,
The Hong Kong Polytechnic University, Hung Hom, Hong Kong, and School of Chemistry,
University of Southampton, Highfield, Southampton SO17 1BJ, United Kingdom

Received: May 23, 2007; In Final Form: July 24, 2007

Complete active space self-consistent field (CASSCF), multireference configuration interaction (MRCI), and restricted-spin coupled-cluster singles−doubles with perturbative triples [RCCSD(T)] calculations have been carried out on low-lying doublet and quartet states of $SnCl_2^+$, employing basis sets of up to aug-cc-pV5Z quality. Effects of core correlation and off-diagonal spin−orbit interaction on computed vertical ionization energies were investigated. The best theoretical estimate of the adiabatic ionization energy (including zero-point vibrational energy correction) to the $\tilde{X}^2A_1$ state of $SnCl_2^+$ is 10.093 ± 0.010 eV. The first photoelectron band of $SnCl_2$ has also been simulated by employing RCCSD(T)/ aug-cc-pV5Z potential energy functions and including Duschinsky rotation and anharmonicity.

Introduction

$SnCl_2$ is important as a precursor in chemical deposition of SnO_2 thin films in the semiconductor gas-sensor industry, and $SnCl_2$/Si mixtures are important as environmentally friendly inorganic fire retardants in polymers. Various other synergic and/or catalytic roles of $SnCl_2$ in synthetic chemistry have been discussed previously (see ref 1 and references therein). As part of a program to obtain more information on low-lying neutral and ionic states of $SnCl_2$, an ab initio study on the low-lying electronic states of $SnCl_2^+$ is reported in this paper.

$SnCl_2$ has been investigated by various types of spectroscopy in the gas phase.[2−15] Among these spectroscopic studies, information on $SnCl_2^+$ can be obtained from the photoelectron (PE) spectrum of $SnCl_2$, which has been recorded on numerous occasions by employment of He I and/or He II radiation or synchrotron radiation[9−13] and from ionization efficiency curves of two electron impact studies.[14,15] However, previous calculations[9,11−13,16−19] performed to characterize low-lying states of $SnCl_2^+$ are of relatively low level (vide infra) by current standards. At the same time, for the low-lying states of $SnCl_2^+$, only the minimum-energy geometries of the $(1)^2A_1$ and $(1)^2B_1$ states has been computed.[17] The present paper reports state-of-the-art ab initio calculations on a large number of low-lying states of $SnCl_2^+$. It is also a continuation of our very recent ab initio study[1] on low-lying electronic states of $SnCl_2$ and simulations of its absorption and single-vibronic-level emission spectra yet to be recorded.

TABLE 1: Basis Sets Used for Sn and Correlated Electrons

basis	ECP28MDF[a]	augmented[b]	correlated
A, A_f,[c] A_{SO}[d]	AVQZ		$5s^25p^2$
A1	AVQZ	2d2f1g	$4d^{10}5s^25p^2$
A2	AVQZ	3s2p2d2f1g	$4s^24p^64d^{10}5s^25p^2$
A3[e]	AVQZ	3s2p2d2f1g	$4s^24p^64d^{10}5s^25p^2$
B	AV5Z		$5s^25p^2$
B1	AV5Z	2d2f1g1h	$4d^{10}5s^25p^2$
B2	AV5Z	2s2p2d1f1g1h	$4s^24p^64d^{10}5s^25p^2$

[a] The standard ECP28MDF_aug-cc-pVQZ (AVQZ) or ECP28MDF_aug-cc-pV5Z (AV5Z) valence basis set[27] was used for Sn, together with the corresponding aug-cc-pV(Q+d)Z {AV(Q+d)} or aug-cc-pV(5+d)Z {AV(5+d)} basis set[28] for Cl (see also footnote *e*). [b] Exponents of these augmented functions are given in ref 1. [c] With the A_f basis set, the g functions in both the basis sets of Sn and Cl were excluded in survey CASSCF calculations. [d] Uncontracted s, p, and d functions of the standard basis sets were used in CASSCF spin−orbit interaction calculations. [e] The standard aug-cc-pwCVQZ basis set[29] was used for Cl, and the $2s^22p^6$ electrons of Cl were also correlated.

Theoretical Considerations and Computational Details. Table 1 summarizes the valence basis sets used for tin, which couple with the fully relativistic small-core effective core potential (ECP), ECP28MDF. This table includes augmented tight functions designed for outer core correlation, and the electrons that were included in the corresponding correlation calculations, for Sn (see footnotes of Table 1 for the corresponding basis sets used for Cl). The computational strategy follows closely that of our previous study on low-lying neutral states of $SnCl_2$.[1] Briefly, initial survey calculations were carried out at the complete active space self-consistent field (CASSCF) and CASSCF/multireference configuration interaction (MRCI) level with a full valence active space employing relatively small basis sets (basis sets A and A_f in Table 1). Further calculations were performed in order to obtain more reliable results by employment of the restricted coupled-cluster singles−doubles with perturbative triples [RCCSD(T)] method and larger basis sets (basis sets A1, A2, A3, B, B1, and B2 in Table 1). These RCCSD(T) calculations investigate effects of core electron correlation of both Sn (basis sets A1, A2, B1 and B2) and Cl (basis set A3) on optimized geometrical parameters and computed relative electronic energies, namely, vertical and adiabatic ionization energies (VIEs and AIEs, respectively). In addition, effects of basis set extension to the complete basis set (CBS) limit on these computed quantities were estimated on

---

* Corresponding authors.

[†] University of Southampton.

[‡] Department of Building Services Engineering, The Hong Kong Polytechnic University.

[§] Department of Applied Biology and Chemical Technology, The Hong Kong Polytechnic University.

10.1021/jp073983w CCC: $37.00

TABLE 2: Computed Vertical Ionization Energies and Largest Computed Configuration Interaction Coefficients for Eight Low-Lying Doublet States of $SnCl_2^+$ [a]

	VIE, eV				
state[b]	CAS[c]/A_f	CAS[d]/A	MRCI[d]/A	MRCI+D[d]/A	$C_0^{MRCI\ b}$
$^2A_1\ (12a_1)^1$	9.15	9.11	9.72	9.89	0.891
$^2B_2\ (9b_2)^1$	9.98	10.05	10.67	10.86	0.752
$^2A_2\ (3a_2)^1$	10.27	10.41	10.95	11.08	0.883
$^2B_1\ (4b_1)^1$	10.81	10.97	11.49	11.62	0.876
$^2A_1\ (11a_1)^1(12a_1)^2$	10.95	11.04	11.59	11.72	0.863
$^2B_2\ (8b_2)^1(9b_2)^2$	11.55	11.65	12.22	12.40	0.728
$^2B_1\ (11a_1)^2(12a_1)^0(4b_1)^2(5b_1)^1$	12.66	12.69	13.41	13.59	0.849
$^2A_2\ (12a_1)^1(4b_1)^2(5b_1)^1(9b_2)^1$	13.02	13.09	13.82	13.99	0.877

[a] Obtained at different levels of calculation: CAS/A_f and CASSCF/MRCI/A calculations were carried out at the RCCSD(T)/A optimized geometry of the $\tilde{X}^1A_1$ state of $SnCl_2$ (from ref 1). [b] With the small-core ECP28MDF ECP accounting for the 1s2s2p3s3p3d shells of Sn, the $\tilde{X}^1A_1$ state of $SnCl_2$ has the valence electronic configuration of ...$(12a_1)^2(4b_1)^2(9b_2)^2(3a_2)^2$. The major open-shell configuration, with the largest computed CI coefficient, C_0^{MRCI}, in the MRCI wavefunction is shown. The computed $\Sigma(C_{ref})^2$ values obtained from the MRCI calculations for all states are larger than 0.93. [c] Average-state CASSCF calculations with eight states: two lowest doublet cationic states of each symmetry of the C_{2v} point group. The computed CASSCF energy of the $\tilde{X}^1A_1$ state of $SnCl_2$ obtained from the eight-state average-state CASSCF/A_f calculations from ref 1 was used to evaluate the VIEs. [d] Two-state CASSCF/MRCI calculations for each symmetry; corresponding energies of the $\tilde{X}^1A_1$ state of $SnCl_2$ from ref 1 were used to evaluate the VIEs. D denotes inclusion of the Davidson correction.

the basis of RCCSD(T) results obtained with basis sets of quadruple-ζ (basis sets A, A1, A2, and A3) and quintuple-ζ (basis sets B, B1, and B2) qualities. Scalar relativistic effects of Sn are assumed to be adequately accounted for by the use of the fully relativistic ECP. Contributions of off-diagonal spin−orbit interaction between the four lowest-lying cationic states to computed VIEs were calculated by employment of average-state CASSCF wavefunctions of the relevant electronic states, spin−orbit pseudopotential of Sn (from the ECP28MDF ECP), and computed RCCSD(T)/A electronic energies for the spin−orbit diagonal elements. Generally, spin−orbit contributions to VIEs were small (they gave an increase of 0.003 eV; vide infra).

The first PE band of $SnCl_2$, which arises from the $SnCl_2^+$ $(\tilde{X}^2A_1) + e \leftarrow SnCl_2\ (\tilde{X}^1A_1)$ ionization process, has been simulated by computed Franck−Condon (FC) factors, which include allowance for Duschinsky rotation and anharmonicity. The RCCSD(T)/B potential energy function (PEF) and the anharmonic vibrational wavefunctions of the $\tilde{X}^1A_1$ state of $SnCl_2$ used to calculate the FC factors of this ionization process are from ref 1. The computed RCCSD(T)/B PEF of the $\tilde{X}^2A_1$ state of $SnCl_2^+$ obtained from the present study is available from the authors. Details of the method employed to calculate FC factors including allowance for Duschinsky rotation and anharmonicity have been described previously (see ref 1 and references therein), and hence are not repeated here. Nevertheless, some technical details specific to calculations of the PEF and anharmonic vibrational wavefunctions of the $\tilde{X}^2A_1$ state of $SnCl_2^+$ are given as follows. The ranges of the bond length r (Sn−Cl), and bond angle θ (Cl−Sn−Cl) used in the RCCSD(T)/B energy scan are $1.77 \leq r \leq 3.50$ Å and $64° \leq \theta \leq 154°$, respectively. A total of 107 RCCSD(T)/B energies were used in the fitting of the PEF. The root-mean-square (rms) deviation of the fitted PEF from computed ab initio energies is 11.9 cm^{-1}. The vibrational quantum numbers of the harmonic basis functions of the symmetric stretching and bending modes of the $\tilde{X}^2A_1$ state of $SnCl_2^+$ employed initially in the calculation of anharmonic wavefunctions have values of up to $v_1 = 10$ and $v_2 = 30$. In addition, a restriction of $(v_1 + v_2) \leq 35$ has been imposed. However, when "hot bands", assuming a Boltzmann distribution for the populations of low-lying vibrational levels of the $\tilde{X}^1A_1$ state of $SnCl_2$ with a vibrational temperature of 300 K, were included in the spectral simulation (vide infra), a larger harmonic basis with v_1, v_2, and $(v_1 + v_2)$ having values of up to 12, 40, and 40 was used.

All ab initio calculations performed in the present study have employed the MOLPRO suite of programs.[20]

Results and Discussion

Ab Initio Results. The results obtained in this work are summarized in Tables 2−6. Since calculations performed here are at significantly higher levels of theory, and more systematic, than previous calculations (see Tables 3−5), the following discussion focuses only on the ab initio results obtained in this study.

Computed Vertical Ionization Energies. Calculated CASSCF/A_f and CASSCF/MRCI/A VIEs for eight lowest-lying doublet states of $SnCl_2^+$ are given in Table 2. The computed MRCI wavefunctions of all these states accessible in the vertical ionization region give a single main reference configuration for each state with a computed CI coefficient C_0^{MRCI} larger than 0.72 (see Table 2), suggesting that a single-reference method should be adequate for these states. (It should be noted also that computed T_1 diagnostics from all RCCSD calculations carried out in the present study on all the doublet and quartet states considered are smaller than 0.0253 and 0.0268, respectively, confirming that nondynamic electron correlation is not important.) From the main electronic configurations of these eight cationic states, it can be seen that, the lowest six can be reached via one-electron ionization processes from the $\tilde{X}^1A_1$ state of $SnCl_2$ (see Table 2, footnote *b*). However, the highest two states, $(2)^2A_1$ and $(2)^2B_2$, are excited states that cannot be studied by the restricted Hartree−Fock-based RCCSD(T) method. Consequently, further RCCSD(T) calculations were performed only on the four lowest cationic states, each of which is the lowest state of each symmetry.

Computed RCCSD(T) VIE values for the lowest four states of $SnCl_2^+$ obtained with different basis sets and core electrons are given in Table 3 together with available theoretical and experimental values for comparison. Considering the computed VIE values for the four lowest cationic states obtained at different levels of calculation in the present study as shown in Table 3, it can be concluded that higher level calculations give larger computed VIE values. This is generally the case, when effects of basis set extension (from QZ to 5Z quality), core correlation, and off-diagonal spin−orbit interaction on the computed RCCSD(T) VIE values are considered. However, without triple excitations, the computed RCCSD VIE values are larger than the computed RCCSD(T) VIE values with the

TABLE 3: Computed Vertical Ionization Energies for Four Low-Lying Doublet States of $SnCl_2^+$ [a]

	VIE, eV				
method	$^2A_1$	$^2B_2$	$^2A_2$	$^2B_1$	ref
MRCI[b]/A	9.86	10.90	11.08	11.71	*c*
MRCI+D[b]/A	10.03	11.07	11.23	11.87	*c*
RCCSD/A	10.14	11.18	11.49	12.01	*c*
RCCSD/A1	10.36	11.31	11.63	12.19	*c*
RCCSD/A2	10.38	11.30	11.62	12.19	*c*
RCCSD/A3	10.39	11.33	11.65	12.22	*c*
RCCSD/B	10.27	11.33	11.64	12.16	*c*
RCCSD/B1	10.39	11.34	11.67	12.24	*c*
RCCSD/B2	10.40	11.34	11.67	12.24	*c*
RCCSD(T)/A	10.22	11.19	11.47	11.97	*c*
RCCSD(T)/A+SO[d]	10.22	11.20	11.48	11.98	*c*
RCCSD(T)/A1	10.34	11.21	11.49	12.03	*c*
RCCSD(T)/A2	10.36	11.20	11.49	12.03	*c*
RCCSD(T)/A3	10.37	11.24	11.53	12.08	*c*
RCCSD(T)/B	10.23	11.23	11.51	12.01	*c*
RCCSD(T)/B1	10.37	11.24	11.53	12.08	*c*
RCCSD(T)/B2	10.38	11.24	11.53	12.08	*c*
best estimate[e]	10.40 ± 0.02	11.30 ± 0.07	11.61 ± 0.07	12.17 ± 0.08	*c*
CNDO	10.72	11.01	11.50	11.82	9
EHMO[f]	8.93	11.27	11.52	11.68	11
ΔSCF/PP[2s2p1d]; (KT)	10.2 (10.6)				16
HF/RPP(4s4p1d) KT[g]	10.36	12.03	12.32	12.88	12
2h-1p CI[h]	8.74	10.15	10.47	10.06	13
electron impact	10.2				15
HeI	10.31[i]		11.31[i]	12.07[i]	10
HeI	10.37	11.0(sh)[j]	11.33	12.12	9
HeI/HeII	10.31	11.27[k]	11.27[k]	12.02[k]	11
HeI/HeII	10.38	11.39[l]	11.39[l]	12.39[l]	12

[a] Obtained at higher levels of calculation: at the RCCSD(T) optimized geometries of the $\tilde{X}^1A_1$ state of $SnCl_2$ with the respective basis sets. [b] Single-state CASSCF/MRCI calculations for each state. D denotes inclusion of the Davidson correction. [c] Present study. [d] See text and footnote *d* of Table 1 for details of spin−orbit (SO) calculations. [e] On the basis of the RCCSD(T)/B2 values, correction to the complete basis set (CBS) limit was estimated by half the difference between values obtained by use of basis sets B2 and A2. Correction of the core correlation of Cl $2s^22p^6$ electrons was estimated by the difference between values obtained by use of the A3 and A2 basis sets. CBS, core correlation, and spin−orbit contributions were assumed to be additive. Maximum theoretical uncertainties given were estimated by differences between the best values and the RCCSD(T)/B2 values. [f] Values are corrected by linear shifts made on the basis of EHMO calculations and a correlation with GeX_2, X = Cl, Br and I; see original work. [g] A relativistic pseudopotential (RPP) and a pseudopotential were used for Sn and Cl, respectively. Uncontracted 4s4d1d Gaussian functions were used for both Sn and Cl. VIEs shown are the negatives of the computed orbital energies. [h] Two-hole one-particle configuration interaction calculations with contracted [9s8p4d] and [6s4p] basis sets for Sn and Cl, respectively; see original work for details. [i] In ref 10, the axes used were such that the b_1 and b_2 irreducible representations of the C_{2v} point group are interchanged as compared with other works. For the sake of consistency with other works, the assignments given here follow those of other works. The assignments of the photoelectron bands observed at 10.31, 11.31, and 12.07 eV given in ref 10 are b_1, $a_2 + a_1$ or $a_2 + b_1$, and $b_1 + b_2$ or $b_1 + a_1$, respectively. [j] Shoulder of the photoelectron band at 11.33 eV. [k] The photoelectron band at 11.27 eV was assigned to both the $(1)^2B_2$ and $(1)^2A_2$ states of $SnCl_2^+$ with computed EHMO IEs of 11.27 and 11.52 eV, respectively. The photoelectron band at 12.02 eV was assigned to both the $(2)^2B_2$ and $(1)^2B_1$ states of $SnCl_2^+$ with computed EHMO IEs of 11.72 and 11.68 eV, respectively. [l] The photoelectron band at 11.39 eV, a double band, was assigned to both the $(1)^2B_2$ and $(1)^2A_2$ states of $SnCl_2^+$ with computed IEs of 12.03 and 12.32 eV, respectively. The photoelectron band at 12.39 eV was assigned to the both the $(1)^2B_1$ and $(2)^2A_1$ states with computed IEs of 12.88 and 13.11 eV, respectively.

same basis sets used, except with basis set A. Nevertheless, on the basis of the more reliable computed RCCSD(T) VIE values, the best computed VIE values to the lowest four cationic states of $SnCl_2^+$ have been estimated and are given in Table 3. These values have included contributions from core correlation, basis set extension to the CBS limit, and off-diagonal spin−orbit interaction (see footnote *e* of Table 3). In addition, the uncertainties associated with the best theoretical VIE values to different states have been estimated and are also given in Table 3.

Comparison between Theory and Experiment: Assignment of the Photoelectron Spectrum of $SnCl_2$. In order to assist assignments of observed photoelectron (PE) bands, computed VIE values are compared with reported experimental values in the following section. However, in the absence of autoionization, it should be noted that the experimental VIE position of a PE band depends on Franck−Condon factors between the neutral and cationic states involved. Unfortunately, available published PE spectra of $SnCl_2$ do not show any resolvable vibrational structure and no AIE position has been reported from these PE studies. Also, reported experimental VIE values from different studies differ by as much as 0.10 eV (see Table 3). Such large differences are most likely due to different calibrants being used for energy calibration, different achievable spectral resolutions of the different spectrometers employed, different experimental conditions employed to produce $SnCl_2$ in the gas phase, and/or complications arising from overlapping PE bands. Nevertheless, computed results shown in Tables 2 and 3 confirm the assignment of the first PE band observed in the He I/II PE spectra of $SnCl_2$ reported previously[9−12] to ionization to the $\tilde{X}^2A_1$ state of $SnCl_2^+$. In addition, our results support the assignment of the ionizations to the $(1)^2B_2$ and $(1)^2A_2$ states both to the observed second PE band, and the assignment of the ionizations to the $(1)^2B_1$ and $(2)^2A_1$ states both to the third PE band. The fourth PE band is then assigned to ionization to the $(2)^2B_2$ state. These assignments agree with those of refs 11−13 but disagree with those of refs 9 and 10.

Regarding the magnitudes of the computed VIE values, for the first PE band of $SnCl_2$, the best theoretical value of 10.40 ± 0.02 eV estimated from the present study agrees very well

TABLE 4: Optimized Geometrical Parameters and Computed Adiabatic Ionization Energies for Four Lowest Doublet States of $SnCl_2^+$ [a]

	$^2A_1$	$^2B_2$	$^2A_2$	$^2B_1$
CASSCF/A_f [b]				
r_e, Å	2.282	2.475	2.509	2.558
θ_e, deg	118.7	66.3	85.6	94.9
AIE, eV	8.72	9.28	10.06	10.59
RCCSD(T)/A [b]				
r_e, Å	2.2886	2.4760	2.4942	2.5334
θ_e, deg	119.25	64.38	82.50	92.87
AIE (RCCSD), eV	9.92	10.35	11.37	11.91
AIE {RCCSD(T)}, eV	9.92	10.30	11.24	11.73
MRSDCI/RECP(3s3p1d) [c]				
r_e, Å	2.241			2.528
θ_e, deg	118.7			93.8
AIE, eV	9.72			11.53

[a] Obtained at the CASSCF/A_f and RCCSD(T)/A levels of calculation. [b] Present study. [c] Reference 16.

with the experimental values of 10.37[9] and 10.38[12] eV. However, the comparison between theoretical and experimental VIE positions of the first PE band of $SnCl_2$ will be further discussed in the later subsection on computed FC factors and simulated spectra. For the VIE of the fourth PE band, when the computed CASSCF/MRCI+D/A value of ca. 12.40 eV is compared with available experimental values of 12.77,[9] 12.72,[10] 12.69,[11] and 12.78[12] eV, the MRCI+D value is too small by ca. 0.30 eV. Nevertheless, it can be seen from Table 3 that, for the computed VIEs to the four lowest states, the computed CASSCF/MRCI+D/A values are smaller than the corresponding best theoretical estimates also by ca. 0.30 eV. Regarding the second and third observed PE bands, each one actually consists of two unresolved bands. Consequently, it is inappropriate to make a direct comparison between the corresponding computed and measured VIE values. Nevertheless, it can be concluded that the above comparison between theory and experiment gives good qualitative agreement.

Optimized Geometrical Parameters and Computed Adiabatic Ionization Energies. Although no experimental AIE position of any PE band of $SnCl_2$ has been reported in the available He I/II PE studies,[9−12] we have estimated the best theoretical AIE value for the first PE band of $SnCl_2$ (see footnote *b* of Table 5) to be 10.09 ± 0.01 eV. This value has included corrections of core electron correlation and basis set extension to the CBS limit. From Table 5, it can be seen that contributions from triple excitations and basis set extension to the computed AIE values are relatively small (<0.02 eV). However, core correlation contributions are considerable, particularly contributions of ca. 0.14 eV from the Sn $4d^{10}$ electrons. Including zero-point vibrational energy correction, the best AIE_0 value is 10.09 eV. This value agrees very well with the experimentally derived value of 10.1 ± 0.4 eV, obtained from the semilog plot of the measured appearance potential in the electron impact study of $SnCl_2 + e \rightarrow SnCl_2^+ + 2e$ of ref 14, and the compiled value of 10.0 eV included in the NIST Chemistry WebBook,[21] estimated from the He I/II PE spectra of $SnCl_2$ of ref 11. However, in view of the rather large uncertainties associated with these two experimentally derived values, it is concluded that the best theoretical AIE obtained here is currently the most reliable value.

The best theoretical r_e and θ_e values of the $\tilde{X}^2A_1$ state of $SnCl_2^+$ have also been derived and they are 2.243 ± 0.008 Å and 119.77 ± 0.03°, respectively (see footnote *b* of Table 5). Similar to the computed AIE values discussed above, basis set extension effects on the computed equilibrium geometrical parameters of the $\tilde{X}^2A_1$ state of $SnCl_2^+$ are small and the major core electron contributions have come from the Sn $4d^{10}$ electrons. By comparison of these values with the corresponding values of the $\tilde{X}^1A_1$ state of $SnCl_2$ (2.341 Å and 97.52° from ref 1), r_e decreases by ca. 0.098 Å while θ_e increases by 22.25° upon ionization. On the basis of these expected geometry changes upon ionization, a long vibrational progression in the bending mode of the cation with a computed fundamental vibrational frequency of 96 cm^{-1} (see Table 5) is expected in the first PE band of $SnCl_2$. In addition, structure in the symmetric stretching mode of the $\tilde{X}^2A_1$ state of $SnCl_2^+$ with a computed fundamental vibrational frequency of 384 cm^{-1} (see Table 5), and also combination bands involving the symmetric stretching and bending modes would also be excited. The vibrational structure of the first PE band of $SnCl_2$ will be further discussed in the subsection on the computed FC factors and simulation of this PE band.

The optimized geometries and computed AIEs for the $\tilde{A}^2B_2$, $\tilde{B}^2A_2$, and $\tilde{C}^2A_1$ states of $SnCl_2^+$ obtained at the RCCSD(T)/A level of calculation are summarized in Table 4. For these three cationic sates, the difference between the computed RCCSD(T)/A AIE and VIE values for the $\tilde{A}^2B_2$ state of $SnCl_2$ of 0.88 eV is particularly large. This is because the $\tilde{A}^2B_2$ state has a very small computed θ_e value of ca. 64°. The PE band to the $\tilde{A}^2B_2$ state should consist of a long vibrational progression in the bending mode and the AIE position should be too weak to be observed because of low Franck−Condon factors in this region.

Low-Lying Quartet States. Computed results for four low-lying quartet states of $SnCl_2^+$ obtained at different levels of calculation are summarized in Table 6. Of course, these quartet states of $SnCl_2^+$ cannot be accessed by a one-electron ionization process from the $\tilde{X}^1A_1$ state of $SnCl_2$. Nevertheless, they have been considered because spin−orbit interaction between doublet and quartet states, which are close in energy, may be significant for a molecule containing a heavy fourth-row element, Sn. Nevertheless, the computed VIE values to these quartet states (electronic energies relative to the $\tilde{X}^1A_1$ state of $SnCl_2$) as shown in Table 6 are larger than ca. 14.4 eV. These quartet states are considerably higher in energy (ca. 2 eV) in the vertical ionization region than the six lowest doublet states, which can be reached via one-electron ionization processes (Table 2). Therefore, it can be concluded that spin−orbit interaction between low-lying doublet and quartet states of $SnCl_2^+$ should be negligibly small, at least in the vertical ionization region.

Computed Franck−Condon Factors and Simulation of the First Photoelectron Band of $SnCl_2$. Some representative simulated spectra of the first PE band, that is, the $\tilde{X}^2A_1 + e \leftarrow \tilde{X}^1A_1$ ionization, of $SnCl_2$ are shown in Figures 1 and 2 (with the relative intensity of the strongest vibrational component set to 100%). The best theoretical estimates of the geometries of the two states involved and the best theoretical AIE_0 value have been used in all the spectral simulations reported here, thus giving the best theoretical PE spectra of $SnCl_2$. In both Figures 1 and 2, each vibrational component has been simulated with the corresponding computed FC factor and a Gaussian line shape. For the two simulated spectra shown in Figure 1, a Boltzmann vibrational temperature of 0 K has been assumed and hence no "hot bands" arising from ionization from vibrationally excited levels of the $\tilde{X}^1A_1$ state of $SnCl_2$ are present in these simulated spectra. For the bottom and top traces of Figure 1, spectral resolutions of 5 meV (ca. 40 cm^{-1}) and 0.5 meV (ca. 4 cm^{-1}) full width at half-maximum (fwhm), respectively, for each vibrational component have been employed. Although previously published He I PE spectra[9−12] of $SnCl_2$ have

TABLE 5: Optimized Geometrical Parameters, Computed Harmonic Vibrational Frequencies, and Computed Adiabatic Ionization Energies for the $\tilde{X}^2A_1$ State of $SnCl_2^+$ [a]

	r_e, Å	θ_e, deg	AIE [RCCSD], eV	AIE [RCCSD(T)], eV	$\omega_1(a_1)$, $\omega_2(a_1)$, $\omega_3(b_2)$
			Present Work		
RCCSD(T)/A	2.289	119.25	9.92	9.92	380.5, 94.3, 418.2
RCCSD(T)/A1	2.261	119.63	10.00	10.05	
RCCSD(T)/A2	2.261	119.62	10.05	10.07	
RCCSD(T)/A3	2.257	119.59	10.06	10.07	
RCCSD(T)/B	2.286	119.19	9.93	9.93	382.4, 94.4, 420.4
RCCSD(T)/B PEF	2.286	119.29			386.5, 96.5
[fundamental frequencies]					[384.3, 96.3]
RCCSD(T)/B1	2.255	119.61	10.05	10.07	
RCCSD(T)/B2	2.251	119.74	10.06	10.08	
best estimate[b]	2.243	119.77	10.07	10.09	
AIE_0[c]				10.09	
			Previous Calculations		
SCF/CI/PP[2s2p1d][d]	2.278	120.3	9.7		
MRSDCI/RECP(3s3p1d)[e]	2.241	118.7	9.72		
LSD[f]	2.322	121.7	9.97		
NLSD-PP[f]	2.365	127.6	9.35		
B3LYP/SDB-aug-cc-pVTZ[g]	2.301	119.4	9.82		
MP2/SDB-aug-cc-pVTZ[g]	2.265	119.4	9.73		

[a] Obtained at the RCCSD(T) level of calculation employing different basis sets (see Table 1). [b] On the basis of the RCCSD(T)/B2 values, correction to the complete basis set (CBS) limit was estimated by half the difference between values obtained by use of basis sets B2 and A2. Correction of the core correlation of Cl $2s^22p^6$ electrons was estimated by the difference between values obtained by use of the A3 and A2 basis sets. CBS and core corrections are assumed to be additive. Estimated theoretical uncertainties are ±0.008 Å, ±0.03 deg, and ±0.01 eV {differences between best estimated values and RCCSD(T)/B2 values}. [c] Including zero-point vibrational corrections, by use of the computed harmonic frequencies obtained at the RCCSD(T)/B level of calculation. [d] Reference 16. [e] Reference 17 [f] Reference 18 [g] Reference 19. The all-electron aug-cc-pVTZ basis set were used for Cl, but f functions were excluded from both basis sets of Sn and Cl.

TABLE 6: Major Electronic Configurations, Corresponding Computed CASSCF Configuration Interaction Coefficients, and Computed Vertical Ionization Energies for Four Low-Lying Quartet States of $SnCl_2^+$ [a]

CASSCF/A_f	$^4A_2$	$^4B_2$	$^4A_1$	$^4B_1$
configuration	$(12a_1)^1(5b_1)^1(9b_2)^1$	$(12a_1)^1(5b_1)^1(3a_2)^1$	$(12a_1)^1(4b_1)^1(5b_1)^1$	$(11a_1)^1(12a_1)^1(5b_1)^1$
CI coefficient	0.945	0.933	0.918	0.916
VIE, eV				
CASSCF/A_f	12.91	13.11	13.46	13.60
RCCSD/A	14.30	14.50	14.90	15.06
RCCSD/B	14.45	14.65	15.06	15.22
RCCSD(T)/A	14.35	14.46	14.83	14.99
RCCSD(T)/B	14.40	14.51	14.88	15.04

[a] Obtained at CASSCF/A_f, RCCSD(T)/A, and RCCSD(T)/B levels of calculation. RCCSD(T) VIEs were computed at RCCSD(T) optimized geometries of the $\tilde{X}^1A_1$ state of $SnCl_2$ with the respective basis sets. For single-state CASSCF/A_f calculations, the RCCSD(T)/A geometry of the $\tilde{X}^1A_1$ state of $SnCl_2$ was used.

considerably lower resolutions (>50 meV fwhm, as estimated from available He I PE spectra) than those of the simulated spectra shown in Figure 1, recent advances in the development of high-resolution spectroscopy (e.g., zero electron kinetic energy-pulsed field ionization (ZEKE-PFI) spectroscopy) have led to reports of milli- to even submillielectronvolt electron energy resolution being achieved in the literature. For examples, resolutions on the order of 6 meV with He I[22] and synchrotron radiation (for electrons with a kinetic energy of up to 50 eV),[23] by use of a hemispherical energy analyzer in each case, have been reported. Recent researches in instrumentation of PE and/or photodetachment spectroscopy show that submillielectronvolt electron energy resolution is achievable.[24−26] In this connection, it is anticipated that a PE spectrum of $SnCl_2$ with a significantly higher resolution than previously reported could be available in the near future. For the two simulated spectra shown in Figure 2, a spectral resolution of 5 meV fwhm has been used. The top and bottom traces in Figure 2 have been simulated with the assumption of Boltzmann distributions for the populations of low-lying vibrational levels of the $\tilde{X}^1A_1$ state of $SnCl_2$ at vibrational temperatures of 300 and 100 K, respectively.

Simulated First PE Band of $SnCl_2$ without "Hot Bands". From Figure 1, it can be seen that the simulated first band of the PE spectrum of $SnCl_2$ spans between ca. 10.17 and 10.70 eV. With a resolution of 5 meV fwhm (bottom trace of Figure 1), the simulated vibrational structure appears to consist of only one vibrational progression. However, with a higher resolution of 0.5 meV fwhm (top trace of Figure 1), it can be seen that the vibrational structure is actually rather complex, involving a large number of vibrational progressions. Computed FC factors show that the strongest vibrational progression is the combination band, $SnCl_2^+$ ($\tilde{X}^2A_1$) $(2,\upsilon_2',0)$−$SnCl_2$ ($\tilde{X}^2A_1$) (0,0,0), with the vibrational component (2,16,0)−(0,0,0) at 10.38 eV having the largest computed FC factor (set to 1.0). Nevertheless, the $(3,\upsilon_2',0)$−(0,0,0), $(1,\upsilon_2',0)$−(0,0,0), $(4,\upsilon_2',0)$−(0,0,0), and $(5,\upsilon_2',0)$−(0,0,0) progressions are also quite strong, with their strongest vibrational components, (3,15,0)−(0,0,0), (1,16,0)−(0,0,0), (4,16,0)−(0,0,0), and (5,15,0)−(0,0,0) at 10.41, 10.33, 10.47, and 10.50 eV having computed FC factors of 0.90, 0.67, 0.56, and 0.51 respectively. In addition, the $(0,\upsilon_2',0)$−(0,0,0) and $(6,\upsilon_2',0)$−(0,0,0) progressions have nonnegligible computed FC factors (>0.01). It should also be noted that the vibrational components, $(5,\upsilon_2'+4,0)$−(0,0,0), $(4,\upsilon_2'+8,0)$−(0,0,0), $(6,v_2',0)$−(0,0,0), $(3,\upsilon_2'+12,0)$−(0,0,0), $(2,v_2'+16,0)$−(0,0,0), $(1,\upsilon_2'+20,0)$−(0,0,0), and $(0,\upsilon_2'+24,0)$−(0,0,0), of the respective vibrational series have very close computed ionization energies (within 0.0027 eV or ca. 22 cm^{-1}). This is because $4\nu_2'$ is roughly equal to ν_1'. Computed FC factors also suggest that the adiabatic

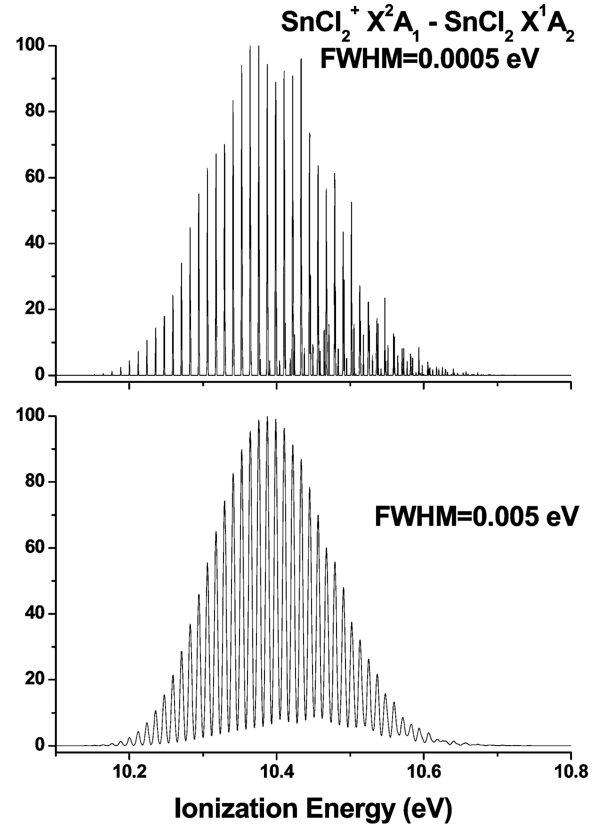

Figure 1. Simulated first photoelectron bands of $SnCl_2$ without "hot bands" (i.e., with a Boltzmann vibrational temperature of 0 K) and with spectral resolutions of 5 (bottom trace) and 0.5 (top trace) meV fwhm; see text.

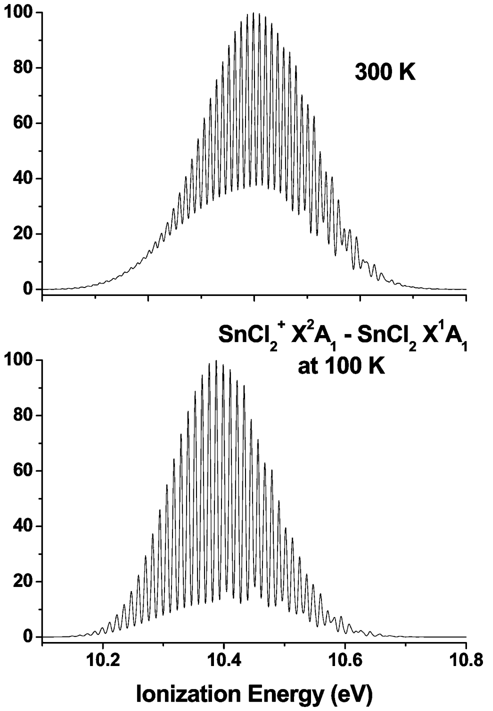

Figure 2. Simulated first photoelectron bands of $SnCl_2$ with a spectral resolution of 5 meV fwhm, with the assumption of Boltzmann distributions for the populations of low-lying vibrational levels of the $\tilde{X}^1A_1$ state of $SnCl_2$ at vibrational temperatures of 100 K (bottom trace) and 300 K (top trace); see text.

region of the first PE band of $SnCl_2$ is too weak to be observed, as the (0,0,0)−(0,0,0) component has a computed FC factor of 2.8×10^{-7}. Without any "hot bands" arising from ionization from excited vibrational levels of the $\tilde{X}^2A_1$ state of $SnCl_2$, the first identifiable vibrational component in the simulated first PE band is probably the (0,7,0)−(0,0,0) component at 10.18 eV.

Regarding the VIE position of the simulated first PE band of $SnCl_2$, with the higher resolution of 0.5 meV fwhm (top trace of Figure 1), the strongest vibrational component, (2,16,0)−(0,0,0), at 10.38 eV may be considered as the VIE position. However, with a lower resolution of 5 meV fwhm (bottom trace of Figure 1), the VIE position, that is, the energy position of the strongest unresolved "peak", is at a slightly higher ionization energy of ca. 10.39 eV. This simulated spectral "peak" at the VIE position consists mainly of contributions from the unresolved vibrational components, (4,9,0)−(0,0,0), (3,13,0)−(0,0,0), (2,17,0)−(0,0,0), and (1,21,0)−(0,0,0), with computed FC factors of 0.13, 0.75, 0.95, and 0.30, respectively. These vibrational components have ionization energies within a 1.5 meV (ca. 11 cm^{-1}) region, because $4\upsilon_2'$ is roughly equal to υ_1', as mentioned above. They cannot be resolved with a spectral resolution of 5 meV.

Simulated First PE Band of $SnCl_2$ Including Hot Bands at Vibrational Temperatures of 100 and 300 K. With a Boltzmann vibrational temperature of 100 K, the simulated first PE band of $SnCl_2$ is shown in the bottom trace of Figure 2. Although the overall vibrational structure of this simulated spectrum is quite similar to that of the simulated spectrum without hot bands (bottom trace of Figure 1), it can be seen that contributions from hot bands have raised the "baseline" of the PE band, when compared with the simulated spectrum without hot bands. Computed FC factors indicate that hot bands at a vibrational temperature of 100 K mainly arise from ionizations from the $SnCl_2$ ($\tilde{X}^2A_1$) (0,1,0) vibrational level, with minor contributions from ionizations from the $SnCl_2$ ($\tilde{X}^2A_1$) (0,2,0) vibrational level. In addition, the major vibrational progressions associated with the hot bands are the $(3,\upsilon_2',0)-(0,1,0)$, $(2,\upsilon_2',0)-(0,1,0)$, $(4,\upsilon_2',0)-(0,1,0)$, $(1,\upsilon_2',0)-(0,010)$, and $(0,\upsilon_2',0)-(0,1,0)$ progressions. Nevertheless, the effects of hot bands at a vibrational temperature of 100 K on the VIE and onset positions of the simulated PE band are small.

The simulated first PE band of $SnCl_2$ with a vibrational temperature of 300 K is shown in the top trace of Figure 2. It can be seen that contributions from hot bands at this vibrational temperature have changed the vibrational structure of the simulated spectrum significantly. In addition to a much stronger rising baseline than that with a vibrational temperature of 100 K, the onset of the PE band is at a lower ionization energy of ca. 10.10 eV, as expected. The first identifiable vibrational feature in the simulated spectrum is possibly due to the vibrational components, (0,6,0)−(1,2,0), (1,3,0)−(0,5,0), and (0,5,0)−(0,3,0) at 10.09, 10.10, and 10.11 eV, with computed FC factors of 0.0012, 0.0013, and 0.0012, respectively. Regarding the VIE position of the simulated PE band, with a vibrational temperature of 300 K and a spectral resolution of 5 meV fwhm, it is now at a higher ionization energy of ca. 10.46 eV. Contributions from hot bands at a vibrational temperature of 300 K are considerably large than those at 100 K, as expected. For example, the computed FC factors of the relatively strong vibrational components of the $(3,\upsilon_2',0)-(0,1,0)$ and $(2,\upsilon_2',0)-(0,1,0)$ progressions are larger than 0.40, and those of the $(2,\upsilon_2',0)-(0,2,0)$ progression are larger than 0.20. Ionizations from higher excited vibrational levels of up to the (2,0,0) level of the $\tilde{X}^2A_1$ state of $SnCl_2$ have smaller, but nonnegligible, contributions to the hot bands. Computed FC factors with a Boltzmann vibrational temperature of 300 K and the simulated spectrum with a resolution of 5 meV fwhm suggest that the unresolved spectral "peak" at the VIE position of 10.46 eV of the first PE band of $SnCl_2$ consists of a large number of vibrational components. The relatively strong ones are (5,11,0)−(0,0,0), (4,15,0)−(0,0,0), (3,19,0)−(0,0,0), (2,23,0)−(0,0,0), (5,12,0)−(0,1,0), (3,20,0)−(0,1,0), (2,24,0)−(0,1,0), (1,28,0)−(0,1,0), (2,25,0)−(0,2,0), (1,29,0)−(0,2,0), (1,30,0)−(0,3,0), and (5,15,0)−(1,0,0), with computed FC factors of 0.13, 0.56, 0.65, 0.25, 0.14, 0.25, 0.36, 0.09, 0.19, 0.13, 0.11, and 0.12, respectively. Comparing the VIE position of 10.46 eV, derived from the simulated first PE band of $SnCl_2$ obtained with a Boltzmann vibrational temperature of 300 K, with available experimental VIE values between 10.31 and 10.38 eV (see Table 3), it appears that the vaporized $SnCl_2$ beams produced when the He I PE spectra were recorded in previous studies have vibrational temperatures of less than 300 K.

Concluding Remarks

State-of-the-art ab initio calculations, which include core correlation, basis set extension to the CBS limit, and off-diagonal spin−orbit coupling, have been carried out on low-lying doublet and quartet states of $SnCl_2^+$. Computed VIEs, which agree well with available experimental values, have been used to confirm/revise assignments of previously reported HeI/II PE spectra. Since no AIE values have been reported in available HeI/II PE studies, it is concluded that the best theoretical AIE_0 value of 10.09 ± 0.01 eV for the ionization to the $\tilde{X}^2A_1$ state of $SnCl_2^+$ obtained in the present study is currently the most reliable value.

The first PE band of $SnCl_2$ has been simulated by employment of computed FC factors, which include allowance for Duschinsky rotation and anharmonicity. The effects of using different vibrational temperatures and/or resolutions in the spectral simulation on the vibrational structure, specifically band onset and VIE positions, and their vibrational assignments derived from the simulated spectra have been investigated. Computed FC factors and simulated spectra show that the vibrational structure of the first PE band of $SnCl_2$ consists of a large number of combination bands involving symmetric stretching and bending modes. In addition, on the basis of computed geometry changes upon ionization and computed FC factors, it is concluded that the AIE vibrational component of the first PE band of $SnCl_2$ would not be identifiable in the simulated spectrum, because of the large change in bond angle upon ionization and its small computed FC factor. Nevertheless, preliminary calculations on the $\tilde{X}^2B_1$ state of $SnCl_2^-$, which give a equilibrium geometry of ca. 2.47 Å and 97°, suggest that the first photodetachment band of $SnCl_2^-$ should consist mainly of a vibrational progression in the symmetric stretching mode of the neutral, and this photodetachment band may reveal the EA position of the $\tilde{X}^1A_1$ state of $SnCl_2$. Calculations on low-lying electronic states of $SnCl_2^-$ and Franck−Condon simulation of its photodetachment spectrum will be reported in a forthcoming article.

Acknowledgment. We are grateful to the Research Committee of the Hong Kong Polytechnic University of HKSAR (Grants G-YF09 and A-PG14) and the Research Grant Council (RGC) of the Hong Kong Special Administrative Region (HKSAR; Grant PolyU 5014/06P) for financial support. The provision of computational resources from the EPSRC (U.K.) National Service for Computational Chemistry Software is also acknowledged.

References and Notes

(1) Lee, E. P. F.; Dyke, J. M.; Mok, D. K. W.; Chow, W. K.; Chau, F.-t. *J. Chem. Phys.* **2007**, *127*, 024308.

(2) Asundi, R. K.; Karim, M.; Samuel, R. *Proc. Phys. Soc.* **1938**, *50*, 581.

(3) Naegli, D.; Palmer, H. B. *J. Mol. Spectrosc*. **1966**, *21*, 325.

(4) Beattie, I. R.; Perry, R.O. *J. Chem. Soc. A* **1970**, 2429.

(5) Nasarenko, A. Y.; Spiridonov, V. P.; Butayev, B. S.; Zasorin, E. Z. *J. Mol. Struct. (THEOCHEM)* **1985**, *119*, 263.

(6) Gershikov, A. G.; Zasorin, E. Z.; Demidov, A. V.; Spiridonov, V. P. *Zh. Strukt. Khim*. **1986**, *27*, 36.

(7) Ermakov, K. V.; Butayev, B. S.; Spiridonov, V. P. *J. Mol. Struct*. **1991**, *248*, 143.

(8) Fields, M.; Devonshire, R.; Edwards, H. G. M.; Fawcett, V. *Spectrochim. Acta A* **1995**, *51*, 2249.

(9) Harris, D. H.; Lappert, M. F.; Pedley, J. B.; Sharp, G. J. *J. Chem. Soc., Dalton Trans*. **1976**, 945.

(10) Evans, S.; Orchard, A. F. *J. Electron Spectrosc. Relat. Phenom*. **1975**, *6*, 207.

(11) Novak, I.; Potts, A. W. *J. Electron Spectrosc. Relat. Phenom*. **1984**, *33*, 1.

(12) Cauletti, C.; de Simone, M.; Stranges, S. *J. Electron Spectrosc. Relat. Phenom*. **1991**, *57*, R1.

(13) Stranges, S.; Adam, M. Y.; Cauletti, C.; de Simone, M.; Furlani, C.; Piancastelli, M. N.; Decleva, A.; Lisini, P. *J. Chem. Phys*. **1992**, *97*, 4764.

(14) Buchanan, A. S.; Knowles, D. J.; Swingler, D. L. *J. Chem. Phys*. **1969**, *73*, 4394.

(15) Knowles, D. J.; Nicholson, A. J. C.; Swingler, D. L. *J. Phys. Chem*. **1970**, *74*, 3642.

(16) Ricart, J. M.; Rubio, J.; Illas, F. *Chem. Phys. Lett*. **1986**, *123*, 528.

(17) Benavidesgarcia, M.; Balasubramanian, K. *J.Chem.Phys*. **1994**, *100*, 2821.

(18) Sicilia, E.; Toscano, M.; Mineva, T.; Russo, N. *Int. J. Quant. Chem*. **1997**, *61*, 571.

(19) Hilpert, K.; Roszak, S.; Saloni, J.; Miller, M.; Lipkowski, P.; Leszczynski, J. *J. Phys. Chem. A* **2005**, *109*, 1286.

(20) MOLPRO is a package of ab initio programs written by H.-J. Werner, P. J. Knowles, R. Lindh, F. R. Manby, M. Schütz, P. Celani, T. Korona, G. Rauhut, R. D. Amos, A. Bernhardsson, A. Berning, D. L. Cooper, M. J. O. Deegan, A. J. Dobbyn, F. Eckert, C. Hampel, G. Hetzer, A. W. Lloyd, S. J. McNicholas, W. Meyer, M. E. Mura, A. Nicklass, P. Palmieri, R. Pitzer, U. Schumann, H. Stoll, A. J. Stone, R. Tarroni, and T. Thorsteinsson.

(21) NIST Standard Reference Database 69, June 2005 Release (http://webbook.nist.gov/chemistry/).

(22) Yencha, A. J.; Baltzer, P.; Cormack, A. J.; Li, Y.; Liebermann, H.-P.; Alekseyev, A. B.; Buenker, R. J. *J. Chem. Phys*. **2003**, *119*, 5943.

(23) Iwai, H.; Namba, H.; Kido, Y.; Taguchi, M.; Oiwa, R. *J. Synchrotron Radiat*. **1998**, 5, 1020.

(24) Giniger, R.; Hippler, T.; Ronen, S.; Cheshnovsky, O. *Rev. Sci. Instrum*. **2001**, *72*, 2543.

(25) Osterwalder, A.; Nee, M. J.; Zhou, J.; Neumark, D. M. *J. Chem. Phys*. **2004**, 121, 6317.

(26) Klar, D.; Ruf, M.-W.; Fabrikant, I. I.; Hotop, H. *J. Phys. B: At. Mol. Opt. Phys*. **2001**, *34*, 3855.

(27) Metz, B.; Stoll, H.; Dolg, M. *J. Chem. Phys*. **2000**, *113*, 2563 (see also the Web site http://www.theochem.uni-stuttgart.de/pseudopotentials/index.en.html).

(28) Peterson, K. A. *J. Chem. Phys*. **2003**, *119*, 11099.

(29) Dunning, T. H., Jr.; Peterson, K. A.; Wilson, A. K. *J. Chem.Phys*. **2001**, *114*, 9244.